Original Article

Distinctive Expression of the Polycomb Group Proteins Bmi1 Polycomb Ring Finger Oncogene and Enhancer of Zeste Homolog 2 in Nonsmall Cell Lung Cancers and Their Clinical and Clinicopathologic Significance

Junko Kikuchi, MD, PhD[1]; Ichiro Kinoshita, MD, PhD[2]; Yasushi Shimizu, MD, PhD[2]; Eiki Kikuchi, MD, PhD[1]; Jun Konishi, MD, PhD[1]; Satoshi Oizumi, MD, PhD[1]; Kichizo Kaga, MD, PhD[3]; Yoshihiro Matsuno, MD, PhD[4]; Masaharu Nishimura, MD, PhD[1]; and Hirotoshi Dosaka-Akita, MD, PhD[2]

BACKGROUND: The polycomb group genes Bmi1 polycomb ring finger oncogene (Bmi1) and enhancer of zeste homolog 2 (EZH2) function as transcriptional repressors involved in gene silencing and in the malignant transformation and biologic aggressiveness of several human carcinomas. In the current study, the authors evaluated Bmi1 and EZH2 protein expression in specimens of human nonsmall cell lung cancer (NSCLC). **METHODS:** The authors conducted an immunohistochemical assessment of 157 surgically resected NSCLCs to evaluate the correlation between Bmi1 and EZH2 expression and various features, including clinical, clinicopathologic, and biologic characteristics. **RESULTS:** Normal bronchial epithelia revealed abundant expression of Bmi1 and sporadic expression of EZH2. Patients who had high EZH2 expression in tumor cells had a poorer prognosis than patients who had low EZH2 expression in tumor cells all pathologic stages of NSCLC (P=.001) and in pathologic stage I NSCLC (P=.006). Multivariate analysis revealed that high EZH2 expression was a independent, unfavorable prognostic factor in patients with pathologic stage I disease (P=.048). High EZH2 expression was correlated significantly with nonadenocarcinoma histology (P=.001), moderate and poor differentiation (P=.001), advanced pathologic tumor classification (P=.02), and high Ki-67 and cyclin E labeling indices ($P < .001$). Bmi1 expression, in contrast, was not a significant prognostic factor and was not correlated with any clinicopathologic factors other than early pathologic tumor classification. **CONCLUSIONS:** Bmi1 and EZH2 had characteristic and distinctive expression in NSCLCs. High EZH2 expression was correlated with tumor aggressiveness and may provide a novel prognostic marker for NSCLCs. ***Cancer* 2010;116:3015–24.** © *2010 American Cancer Society.*

KEYWORDS: polycomb group protein, Bmi1, EZH2, nonsmall cell lung cancer, immunohistochemistry.

Lung cancer is a leading cause of cancer death worldwide, and nonsmall cell lung cancer (NSCLC) accounts for >80% of all lung cancers. Despite some advances in early detection and recent improvements in treatment, the prognosis for patients with lung cancer remains poor.[1,2] The current challenge is to identify new therapeutic targets and strategies and to incorporate them into existing treatment regimens with the objective of improving therapeutic gain. Identifying reliable markers predictive of clinical outcome also would aid in establishing therapeutic strategies and selecting treatment options for each patient with NSCLC.

Epigenetic gene silencing is an important mechanism for the loss of gene function and collaborates with genetic mutation in the initiation and progression of human cancer. Polycomb group (PcG) proteins regulate epigenetically mediated transcriptional silencing.[3] They are involved in the maintenance of embryonic and adult stem cells and the repression of key tumor-suppressor pathways, which may contribute to their oncogenic function.[4] PcG proteins function in distinct

Corresponding author: Ichiro Kinoshita, MD, PhD, Department of Medical Oncology, Hokkaido University Graduate School of Medicine, North 15, West 7, Kita-ku, Sapporo 060-8638, Japan; Fax: (011) 81-11-706-5077; kinoshii@med.hokudai.ac.jp

[1]First Department of Medicine, Hokkaido University School of Medicine, Sapporo, Japan; [2]Department of Medical Oncology, Hokkaido University Graduate School of Medicine, Sapporo, Japan; [3]Department of Surgical Oncology, Hokkaido University Graduate School of Medicine, Sapporo, Japan; [4]Department of Surgical Pathology, Hokkaido University Hospital, Sapporo, Japan

DOI: 10.1002/cncr.25128, **Received:** September 8, 2009; **Revised:** October 23, 2009; **Accepted:** October 23, 2009, **Published online** March 30, 2010 in Wiley InterScience (www.interscience.wiley.com)

multiprotein complexes that can be distinguished roughly into 1 complex involved in silencing initiation (polycomb repressive complex 2 [PRC2]) and another complex involved in the maintenance of gene silencing (PRC1).[5,6]

The Bmi1 polycomb ring finger oncogene (Bmi1), a key component of the PRC1 complex, was identified initially as an oncogene that cooperates with *c-myc* in the generation of B-cell lymphoma.[7,8] The oncogenic potential of Bmi1 is caused in part by its negative regulation of the *Ink4alArf* locus, which encodes 2 proteins ($p16^{INK4a}$ and $p19^{ARF}$) that suppress proliferation and promote apoptosis,[9,10] and its role in stem cell maintenance.[11,12] Elevated expression of Bmi1 has been reported in multiple types of cancers, including oral cancer,[13] lymphoma,[14,15] and breast cancer.[16,17] In previous studies on NSCLC, normal bronchial epithelial cells had abundant Bmi1 expression, whereas tumor cells had various expression patterns.[18,19] Vrzalikova et al reported that high Bmi1 expression was correlated with advanced stage and with poor disease-free survival in patients with early stage NSCLC who had received adjuvant chemotherapy,[20] whereas another group reported no association between Bmi1 expression and tumor characteristics (proliferation rate, differentiation, size, histology) or prognosis.[18] Thus, the clinical and clinicopathologic value of Bmi1 in NSCLC remains controversial.

The enhancer of zeste homologue 2 (EZH2), a key component of the PRC2 complex, possesses histone methyltransferase activity and causes methylation at lysine residues of histone H3. Previous investigators have reported that EZH2 is overexpressed in aggressive prostate cancer,[21] breast cancer,[22] bronchial squamous cell cancer,[19] melanoma,[23] bladder cancer,[24] liver cancer,[25] and gastric cancer.[26] EZH2 expression levels correlate with aggressiveness, metastasis, and a poor prognosis.[21-23] However, to our knowledge, there have been no studies evaluating EZH2 expression and its correlation with clinical and clinicopathologic features in a large cohort of patients with NSCLC.

A recent study indicated that tumors with dual-positive, Bmi1/EZH2 high-expressing prostate cancer cells manifest clinically aggressive disease phenotypes and are significantly more likely to recur after radical prostatectomy.[27] The objective of the current study was to investigate expression of both Bmi1 and EZH2 proteins by immunohistochemistry in a series of NSCLC and to analyze the correlation between these proteins and various features, including clinical and clinicopathologic parameters, cell biologic characteristics, and patient outcomes.

MATERIALS AND METHODS

Tumor Specimens and Survival Data

The current study included 157 consecutive patients (106 men and 51 women) who had adequate archival primary tumor specimens obtained during radical surgery at Hokkaido University Medical Hospital between 1982 and 1994. Histologic diagnoses and grades of differentiation were determined in accordance with 1982 World Health Organization criteria. Specimens included 65 squamous cell carcinomas, 82 adenocarcinomas, 2 large cell carcinomas, and 7 adenosquamous cell carcinomas. For this study, nonadenocarcinomas included squamous cell carcinomas, large cell carcinoma, and adenosquamous cell carcinoma. The pathologic stage (pStage) was based on the American Joint Committee on Cancer guidelines for postoperative tumor-lymph node-metastasis (TNM) classification.[28] The specimens represented pStage I tumors ($n = 91$), pStage II tumors ($n = 23$), pStage III tumors ($n = 40$), and pStage IV tumors ($n = 3$). Survival was analyzed for the 145 patients who 1) survived for >3 months after surgery, 2) did not die of causes other than lung cancer within 5 years after surgery, and 3) were followed for >3 years after surgery (for patients who remained alive). Ninety patients and 67 patients survived for >3 years and for >5 years, respectively, in all pStages; and 62 patients and 53 patients survived for >3 years and for >5 years, respectively, with pStage I disease. Survival data were updated in May 2006, and the median follow-up among the patients who remained alive was 3349 days (range, 1184-5830 days). Informed consent was obtained from all patients. This study was approved by the Medical Ethical Committee of Hokkaido University School of Medicine.

Immunohistochemical Analysis

Bmi1 and EZH2 expression was analyzed by immunohistochemistry. The labeled streptavidin-biotin method was used on 4-μm sections of formalin-fixed, paraffin-embedded tissue after deparaffinization. Briefly, deparaffinized tissue sections were treated in 10 mM citrate buffer, pH 6.0, for 20 minutes at 121°C in an autoclave to retrieve the antigenicity. Next, the sections were immersed in methanol containing 1.5% hydrogen peroxide for 20 minutes to block endogenous peroxidase activity then incubated with normal rabbit serum to block the nonspecific antibody binding sites. The sections were reacted consecutively with mouse monoclonal anti-Bmi1 antibody (F6; Upstate Laboratories, Albany, NY)[18] or anti-

EZH2 antibody (11/EZH2; BD Transduction Laboratories, Mississauga, ON, Canada)[29] at dilutions of 1:150 and 1:100, respectively, at 4°C overnight. Immunostaining was performed by using the biotin-streptavidin immunoperoxidase method with 3,3-diaminobenzidine as a chromogen (SAB-PO kit; Nichirei, Tokyo, Japan). Hematoxylin solution was used for counterstaining. One sample that was positive for either Bmi1 or EZH2 was included as a positive external control with each batch of staining. The immunohistochemical evaluations were assessed twice by 1 investigator (J.K.) using a BX 40 microscope (Olympus, Tokyo, Japan) who was blinded to the status of other immunohistologic and clinical data.

Western Blot Analysis

Lysates of NSCLC cell lines and tumor tissues were prepared by lysing the cells and tissues in radioimmune precipitation assay buffer (150 mM NaCl; 1% Triton X-100; 1% deoxycholate; 0.1% sodium dodecyl sulfate [SDS]; 10 mM Tris, pH 7.4) supplemented with 100 μg/mL leupeptin, 100 μg/mL aprotinin, and 10 mM phenylmethylsulfonyl fluoride. The cell lysates were sonicated and centrifuged to remove debris, and protein concentrations were determined using the Bio-Rad Protein Assay kit (Bio-Rad Laboratories, Hercules, Calif). Equal amounts of protein were separated on 12% or 15% SDS gels, transferred onto nitrocellulose membranes (Amersham Biosciences, Inc. St. Albans, United Kingdom), and incubated with the following antibodies: anti-Bmi1 antibody (F6; Upstate Laboratories), anti-EZH2 antibody (11/EZH2; BD Transduction Laboratories), and antiactin antibody (A-2066; Sigma-Aldrich Company, St. Louis, Mo). Total cell extracts from A549 cells and nuclear extracts from Jurkat cells were used as positive controls for Bmi1[18] and EZH2, respectively.[30] The primary antibodies were detected using antirabbit or antimouse antibody conjugated with horseradish peroxidase (NA934V and NA931V, respectively; Amersham Biosciences Inc.) and were observed using the Amersham ECL system after washing with Tris-buffered saline/Tween-20 6 times for 5 minutes each after incubation in the first and second antibodies.

Statistical Analysis

The associations between Bmi1 or EZH2 expression and categorical variables were analyzed by using chi-square tests or Fisher exact tests, as appropriate. Multivariate logistic regression analysis was used to assess the effect of more than 1 factor on EZH2 expression. Survival curves were estimated using the Kaplan-Meier method, and differences in survival distributions were evaluated by using the log-rank test. Univariate and multivariate analyses using Cox proportional hazards modeling was applied to measure correlations between various factors and overall survival. The level of significance was set at $P < .05$. Statistical analyses were done using SPSS software (version 11.0; SPSS Inc., Chicago, Ill).

RESULTS

First, we tested the quality of antibodies that were used in the current study by Western blot analysis and immunohistochemistry using NSCLC cell lines and surgical specimens. Western blot analysis detected Bmi1 and EZH2 proteins as bands with molecular weights of 45 kDa and 91 kDa, respectively (Fig. 1A). All 4 NSCLC cell lines revealed abundant expression of both proteins. In 3 surgical specimens from the study cohort of NSCLCs, Bmi1 and EZH2 expression was detected to various degrees, consistent with the immunohistochemical staining results (Fig. 1A).

Expression of Bmi1 and EZH2 in NSCLCs was located primarily in the nuclei by immunohistochemistry in surgical specimens, and some specimens also had partial cytoplasmic staining with a nuclear-dominant pattern (Fig. 1B,C). These observations were in agreement with a previously reported study.[31] In normal bronchial epithelial cells, moderate-to-strong nuclear expression of Bmi1 was observed in >50% of basal cells, ciliated cells, and mucinous goblet cells. Sporadic expression of EZH2 at various intensities was observed in basal cells and ciliated cells, consistent with a previously report.[19] Observation of normal alveolar pneumocytes revealed sporadic nuclear expression of Bmi1 but not EZH2. Because both proteins function in the nucleus and actually have such nuclear-dominant expression, only nuclear expression was taken into account in the scoring system that was used.

High Bmi1 expression was defined as >10% of nuclear staining at moderate-to-strong intensity using a previously described scoring system.[32] High Bmi1 expression was observed in 56 NSCLCs (36%). High Bmi1 expression was significantly more prevalent in pathologic T1 (pT1) tumors than in pT2, pT3, or pT4 tumors ($P = .005$; chi-square test), whereas no other clinical or clinicopathologic parameters were correlated with Bmi1 expression (Table 1). Because abundant expression of Bmi1 was observed in normal bronchial epithelial cells, we also used a cutoff level of 50% of nuclear staining in

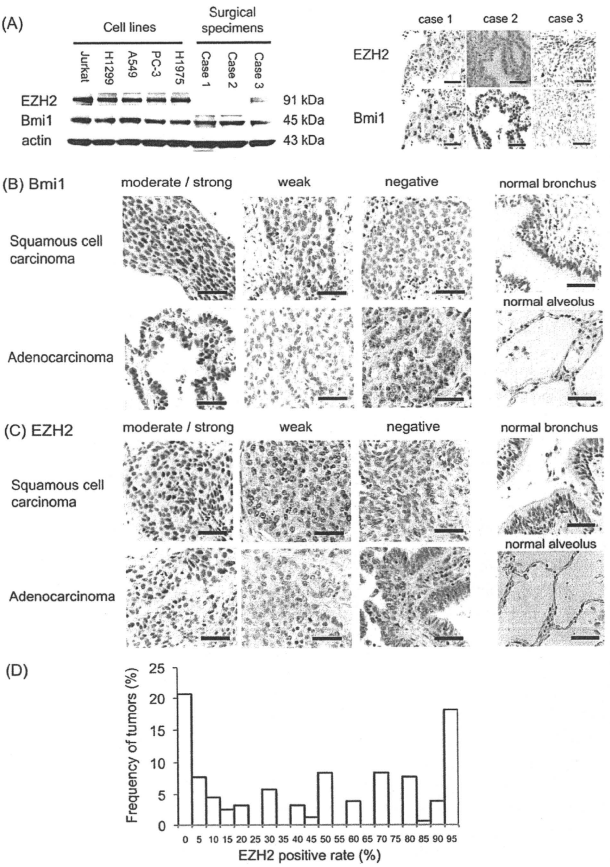

Figure 1. (A) Western blot analysis revealed Bmi1 polycomb ring finger oncogene (Bmi1) and enhancer of zeste homologue 2 (EZH2) expression in nonsmall cell lung cancer (NSCLC) cell lines and surgical specimens from 3 patients in the current cohort. Bmi1 and EZH2 proteins were detected as bands with a molecular weight of 45 kDa and 91 kDa, respectively. All 4 NSCLC cell lines had abundant expression of both proteins. In 3 surgical specimens, Bmi1 expression was detected strongly in Cases 1 and 2 and modestly in Case 3, and EZH2 expression was detected substantially in Case 3 and faintly in Cases 1 and 2, consistent with the results from immunohistochemical staining. Total cell extracts from A549 cells and nuclear extracts from Jurkat cells were used as positive controls for Bmi1 and EZH2, respectively. (B,C) Immunohistochemical staining patterns are shown for Bmi1 and EZH2 in NSCLC. NSCLC specimens were stained with (B) anti-Bmi1 antibody or (C) anti-EZH2 antibody. Bmi1 and EZH2 expression in normal bronchial and alveolar cells also is shown (scale bar = 50 μm). (D) This histogram illustrates the distribution of nuclear EZH2 expression of any intensity in 157 NSCLC specimens that studied in the current study.

Table 1. Relation Between Expression of the Polycomb Group Proteins Bmi1 and EZH2 and Clinical and Clinicopathologic Characteristics in 157 Patients With Surgically Resected Nonsmall Cell Lung Cancer

	Bmi1 Expression			EZH2 Expression		
	No. of Patients			No. of Patients		
Characteristic	Low	High	*P*	Low	High	*P*
Age, y						
<65	50	25	.7	33	41	.1
≥65	51	30		26	54	
Sex						
Men	70	36	.6	25	79	<.001
Women	31	20		34	17	
Smoking history						
Nonsmoker	27	16	1.0	31	11	<.001
Smoker, pack-y	64	36		24	74	
<20	27	22	.1	32	17	<.001
≥20	64	29		23	68	
Histology						
Adeno	51	31	.06	49	33	<.001
Squamous	40	25		7	56	
Other[a]	9	0		2	7	
Differentiation						
Well differentiated	27	16	.9	31	12	<.001
Moderately differentiated	40	24		15	48	
Poorly differentiated	22	15		6	30	
Pathologic tumor classification						
T1	20	23	.005	22	19	.02
T2-T4	81	32		37	76	
Pathologic lymph node status						
N0	65	38	.6	40	61	.7
N1-N3	36	17		19	34	
Pathologic disease stage						
I	56	35	.5	37	52	.3
II-IV	43	20	—	21	42	—

Bmi1 indicates Bmi1 polycomb ring finger oncogene; EZH2, enhancer of zeste homolog 2; Adeno, adenocarcinoma; Squamous, squamous cell carcinoma.
[a] Other indicates large cell carcinoma and adenosquamous cell carcinoma.

tumor cells. High Bmi1 expression also was observed in 23 NSCLCs (15%), and similar results were obtained, including a correlation with pT classification ($P < .001$; data not shown).

The histogram in Figure 1D illustrates the distribution of nuclear EZH2 expression of any intensity in all 157 NSCLC specimens in the current study. The median positive staining rate of EZH2 was 30%. The tumors were divided into 2 groups with a cutoff level of 25% of any nuclear staining according to a previously validated scoring system in which high EZH2 expression was correlated with prognosis in patients with breast cancer and prostate cancer.[21,22] High EZH2 expression was observed in 96 NSCLCs (62%). The chi-square test revealed that high EZH2 expression was significantly more prevalent in tumors from men versus tumors from women ($P < .001$); in tumors from smokers versus tumors from nonsmokers ($P < .001$); in nonadenocarcinomas versus adenocarcinomas ($P < .001$); in moderately and poorly differentiated tumors versus well differentiated tumors ($P < .001$); and in pT2, pT3, and T4 tumors versus pT1 tumors ($P = .02$). EZH2 expression was not associated with pathologic lymph node (pN) status or and pStage (Table 1). Multivariate logistic regression analysis for the correlation between EZH2 expression and various characteristics revealed a significant association of high EZH2 expression

with nonadenocarcinoma ($P = .001$) and with moderate and poor differentiation ($P = .02$) (Table 2).

Among biologic characteristics of the tumors that were studied previously in the same cohort of

Table 2. Multivariate Logistic Regression Analysis for the Correlation Between EZH2 Expression and Clinical and Clinicopathologic Characteristics

Variable[a]	Adjusted OR (95% CI)	P
Sex: Men vs women	4.57 (0.83-25.0)	.1
Smoking history : ≥20 Pack-y vs <20 pack-y	1.28 (0.23-7.01)	.8
Histology: Nonadenocarcinoma[b] vs adenocarcinoma	5.62 (2.01-15.6)	.001
Differentiation: Moderately and poorly vs well differentiated	3.43 (1.24-9.46)	.02
Pathologic tumor classification: T2-T4 vsT1	1.87 (0.65-5.40)	.2

OR indicates odds ratio; 95% CI, 95% confidence interval.
[a] These variables were selected from Table 1, because they were correlated significantly with enhancer of zeste homolog 2 (EZH2) expression in univariate analysis.
[b] Included squamous cell carcinoma, large cell carcinoma, and adenosquamous cell carcinoma.

Table 3. Relation Between EZH2 Expression and Cellular Biologic Characteristics

Characteristic	EZH2 Expression, % Low	High	P
Bmi1 expression			
High	28	55	.3
Low	31	41	
Ki-67 expression			
High[a]	18	75	<.001
Low	36	17	
p27^{KIP1} Expression			
High[b]	43	83	.3
Low	8	9	
Cyclin E expression			
High[c]	20	61	<.001
Low	34	32	

EZH2 indicates enhancer of zeste homolog 2; Bmi1, Bmi1 polycomb ring finger oncogene.
[a] Ki-67 high indicates labeling indices ≥30%.
[b] p27 High indicates labeling indices ≥5%.
[c] Cyclin E high indicates labeling indices ≥30%.

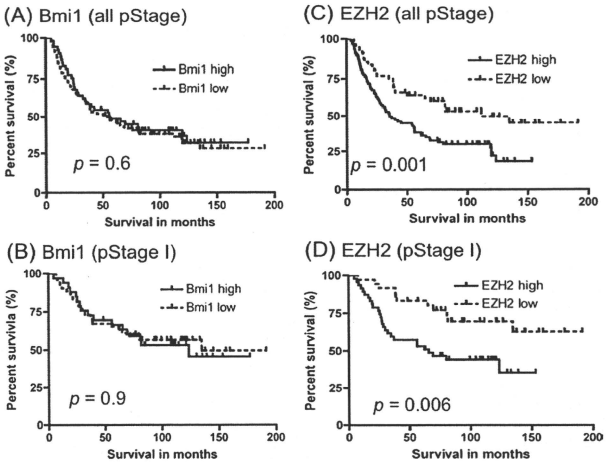

Figure 2. These Kaplan-Meier survival curves illustrate the survival of patients with nonsmall cell lung cancer (NSCLC) who underwent radical resection. Survival curves were stratified by the expression of (A,B) the Bmi1 polycomb ring finger oncogene (Bmi1) and (C,D) enhancer of zeste homologue 2 (EZH2) for (A,C) all patients with NSCLC (n = 145) and (B,D) patients with pathologic stage I disease (n = 83). EZH2 expression was correlated with shorter survival both in all patients and patients with pathologic stage I disease, whereas Bmi1 expression had no impact on survival.

Table 4. Univariate and Multivariate Analyses Using the Cox Proportional Hazards Model for Clinical and Clinicopathologic Factors That Affected Overall Survival After Nonsmall Cell Lung Cancer (NSCLC) Resection for NSCLC

Variable	HR (95% CI)[a]	P
Univariate analysis		
Sex: Women vs men	0.64 (0.40-0.99)	.050
Age: ≥65 y vs <65 y	1.40 (0.93-2.11)	.1
Smoking history: ≥20 Pack-y vs <20 pack-y	0.78 (0.41-1.95)	.8
Histology: Adenocarcinoma vs nonadenocarcinoma[b]	0.75 (0.50-1.12)	.2
Differentiation: Moderately and poorly differentiated vs well differentiated	2.29 (1.34-3.91)	.002
Bmi1 expression: High vs low	1.14 (0.76-1.72)	.5
EZH2 expression: High vs low	2.08 (1.32-3.23)	.002
Pathologic tumor classification: T2-T4 vs T1	1.73 (1.05-2.84)	.03
Pathologic lymph node status: N1-N2 vs N0	2.93 (1.94-4.44)	<.001
Pathologic disease stage II-IV vs I	3.25 (2.13-4.96)	<.001
Multivariate analysis[a]		
Sex: Women vs men	0.93 (0.53-1.63)	.8
Differentiation: Moderately and poorly differentiated vs well differentiated	1.49 (0.79-2.80)	.2
EZH2 expression: High vs low	1.59 (0.86-2.94)	.1
Pathologic tumor classification: T2-T4 vs T1	0.96 (0.54-1.71)	.9
Pathologic lymph node status: N1-N2 vs N0	2.76 (1.74-4.37	<.001

HR indicates hazard ratio; CI, confidence interval; Bmi1, Bmi1 polycomb ring finger oncogene; EZH2, enhancer of zeste homolog 2.
[a] This variable was selected for multivariate analysis because it was a significant prognostic factor on univariate analysis.
[b] Included squamous cell carcinoma, large cell carcinoma, and adenosquamous cell carcinoma.

NSCLCs,[33,34] high Ki-67 and cyclin E expression levels were correlated with high EZH2 expression ($P < .001$) (Table 3), whereas Bmi1 expression was not correlated with either characteristic (data not shown). There was no association between Bmi1 expression and EZH2 expression (Table 3).

Next, we analyzed the relation between Bmi1 or EZH2 expression and survival in 145 patients who met the criteria described above for survival analysis (see the Materials and Methods) (Fig. 2). Bmi1 expression was not associated with survival among patients in all pStages or in patients with pStage I disease (Fig. 2A,B). In the entire cohort, patients who had tumors with high EZH2 expression had shorter survival than patients who had tumors with low expression ($P = .001$) (Fig. 2C). In the group of 83 patients with pStage I NSCLC, patients who had tumors with high EZH2 expression also had shorter survival ($P = .006$) (Fig. 2D). The importance of EZH2 as a prognostic factor was analyzed next in a Cox proportional hazards model analysis of all patients. In univariate analysis of potential prognostic factors, high EZH2 expression and moderate/poor differentiation, advanced pathologic tumor (pT) and pN classifications, and advanced pStage were significant, unfavorable prognostic factors (Table 4). In multivariate analysis, only advanced pN classification was a significant and independent, unfavorable prognostic factor ($P < .001$) (Table 4). In patients with pStage I NSCLC, high EZH2 expression was a significant, unfavorable prognostic factor ($P = .008$) (Table 5). In multivariate analysis, high EZH2 expression was the only significant and independent, unfavorable prognostic factor ($P = .048$) (Table 5)

Table 5. Univariate and Multivariate Analyses Using the Cox Proportional Hazards Model for Clinical and Clinicopathologic Factors That Affected Overall Survival After Nonsmall Cell Lung Cancer (NSCLC) Resection for Patients With Pathological Stage I NSCLC (n=83)

Variable	HR (95% CI)	P
Univariate analysis		
Sex: Women vs men	0.55 (0.28-1.11)	.1
Age: ≥65 y vs <65 y	1.82 (0.96-3.48)	.07
Smoking history: ≥20 Pack-y vs <20 pack-y	1.17 (0.30-4.51)	.8
Histology: Adenocarcinoma vs nonadenocarcinoma[a]	0.53 (0.28-1.01)	.053
Differentiation: Moderately and poorly differentiated vs well differentiated	1.88 (0.90-3.90)	.09
Bmi1 expression: High vs low	1.05 (0.56-1.99)	.88
EZH2 expression: High vs low	2.63 (1.30-5.26)	.008
Pathologic tumor classification: T2-T4 vs T1	1.07 (0.57-2.03)	.8
Multivariate analysis		
Age: ≥65 y vs <65 y	1.45 (0.74-2.84)	.3
Histology: Adenocarcinoma vs nonadenocarcinoma[a]	0.86 (0.39-1.94)	.7
EZH2 expression: High vs low	2.56 (1.01-6.67)	.048
Differentiation: Moderately and poorly differentiated vs well differentiated	1.00 (0.40-2.52)	1.0

HR indicates hazard ratio; CI, confidence interval; Bmi1, Bmi1 polycomb ring finger oncogene; EZH2, enhancer of zeste homolog 2.
[a] Included squamous cell carcinoma, large cell carcinoma, and adenosquamous cell carcinoma.

DISCUSSION

In the current study, we examined expression levels of the PcG proteins Bmi1 and EZH2 in NSCLC and demonstrated a positive correlation between high EZH2 expression and poor patient prognosis, nonadenocarcinoma histology, moderate and poor differentiation, and cell proliferation. Likewise, in patients with prostate cancer,

increased EZH2 expression has been correlated with aggressive tumor behavior and poor survival.[21] In addition, high EZH2 protein expression has been observed in several other malignant tumors, and its expression has been correlated with recurrence, aggressiveness, metastatic potential, and poor survival in patients breast cancer, melanoma, uterine cancer, and gastric cancer.[23,26] The correlation between high EZH2 expression and tumor aggressiveness and poor survival in those studies is in good agreement with our current observations in NSCLC.

The correlation of EZH2 with Ki-67 and cyclin E observed in the current study is consistent with experimental data indicating that EZH2 plays a role in cell cycle regulation and proliferation.[35,36] A previous report indicated that activated p53 suppressed EZH2 gene expression, and p53-dependent suppression of EZH2 expression contributed to p53-mediated G2/M arrest.[36] In addition, a significant association was observed between EZH2 and tumor cell proliferation, as estimated by Ki-67 expression and mitotic counts, in several tumors.[23] These findings, including ours, suggest that EZH2 may be a useful marker for cell proliferation activity in NSCLC.

Because nonadenocarcinomas were more prevalent in men who smoked, high EZH2 expression in nonadenocarcinoma may be related to sex or to the use of tobacco. Recently, Hussain et al reported that tobacco smoke engaged polycomb repressor complexes that contained EZH2 to mediate epigenetic silencing of Dickkopf-1 (a Wnt signaling antagonist) and enhanced the malignant phenotype of lung cancer cells.[37]

Although the mechanism by which EZH2 mediates tumor aggressiveness is unclear, recent studies indicate that EZH2 mediates transcriptional silencing of a tumor suppressor gene E-cadherin (by trimethylation of H3 lysine 27).[38,39] Yu et al demonstrated that EZH2 may mediate increased invasiveness and metastasis by silencing several downstream targets in addition to E-cadherin, including the adrenergic receptor (ADR) ADRB2.[40]

Tan et al identified 3-deazaneplanocin A (DZNep), which is a small molecule that inhibits the expression of PRC2 complex proteins containing EZH2 and induces apoptotic cell death together with histone deacetylase (HDAC) inhibitors in cancer cells, but not in normal cells.[41] Taken together with high expression of EZH2 in NSCLC cells and its association with aggressive phenotypes, PRC2 inhibitors like DZNep, which, together with HDAC inhibitor, pharmacologically reverses cancer-associated epigenetic gene repression, may provide potent therapy for NSCLC.

The inverse correlation between Bmi1 expression and pT classification was unexpected because of its oncogenic potential, including its negative regulation of the *Ink4aIArf* locus[9,10] and its role in stem cell maintenance.[11,12] In previous NSCLC studies, Vonlanthen et al[18] reported no association of Bmi1 expression with tumor characteristics (proliferation rate, differentiation, and size) or prognosis, whereas Vrzalikova et al[20] reported that Bmi1 expression was correlated with advanced stage and poor disease-free survival, but not with overall survival. For other types of cancer, some studies demonstrated that overexpression of Bmi1 was correlated with a poor prognosis[42-44]; however, others reported that loss of Bmi1 expression was correlated with an aggressive phenotype, indicating a protective role of the Bmi1 protein.[45-47] Abundant expression of Bmi1 in normal bronchial epithelial cells in the current study and in a previous report[19] and low Bmi1 expression in the majority of tumor cells suggest that Bmi1 may have a protective role in NSCLC. The role of Bmi1 in lung cancer remains to be defined.

Although a recent study indicated that tumors with dual-positive, Bmi1/EZH2 high-expressing prostate cancer cells manifest aggressive disease phenotypes,[27] no association between Bmi1 and EZH2 expression and no significant effect of Bmi1 on aggressive disease phenotypes were observed in the current study. In other types of cancer, expression of Bmi1 and EZH2 diverged during normal B-cell development, whereas Hodgkin/Reed-Sternberg cells coexpressed Bmi1 and EZH2.[30] EZH2 and Bmi1 may cooperate in the initiation and progression of hepatocellular carcinoma.[48] In breast cancer, although EZH2 overexpression correlates with a poor prognosis, Bmi1 overexpression correlates with a good outcome.[49] In lung cancer, Breuer et al[19] reported increased expression of EZH2 in Bmi1-positive neoplastic cells in bronchial squamous cell carcinomas from 7 patients and premalignant precursor lesions, whereas normal bronchial epithelium had widespread expression of Bmi1 in EZH2-negative cells. To our knowledge, ours is the first study to examine Bmi1 and EZH2 expression in a large number of patients with NSCLC. The distinctive expression patterns that we observed suggest that expression may have different functional consequences for NSCLC.

In conclusion, Bmi1 and EZH2 have characteristic and distinctive expression in NSCLC. High EZH2 expression is correlated with tumor aggressiveness and may provide a novel prognostic marker of NSCLC.

CONFLICT OF INTEREST DISCLOSURES

The authors made no disclosures.

REFERENCES

1. Parkin DM. Global cancer statistics in the year 2000. *Lancet Oncol.* 2001;2:533-543.
2. Jemal A, Siegel R, Ward E, et al. Cancer statistics, 2009. *CA Cancer J Clin.* 2009;59:225-249.
3. Ringrose L, Paro R. Epigenetic regulation of cellular memory by the polycomb and trithorax group proteins. *Annu Rev Genet.* 2004;38:413-443.
4. Sparmann A, van Lohuizen M. Polycomb silencers control cell fate, development and cancer. *Nat Rev Cancer.* 2006; 6:846-856.
5. Lund AH, van Lohuizen M. Polycomb complexes and silencing mechanisms. *Curr Opin Cell Biol.* 2004;16:239-246.
6. Levine SS, King IF, Kingston RE. Division of labor in polycomb group repression. *Trends Biochem Sci.* 2004;29:478-485.
7. van Lohuizen M, Verbeek S, Scheijen B, et al. Identification of cooperating oncogenes in E mu-myc transgenic mice by provirus tagging. *Cell.* 1991;65:737-752.
8. Haupt Y, Alexander WS, Barri G, et al. Novel zinc finger gene implicated as myc collaborator by retrovirally accelerated lymphomagenesis in E mu-myc transgenic mice. *Cell.* 1991;65:753-763.
9. Jacobs JJ, Scheijen B, Voncken JW, et al. Bmi-1 collaborates with c-Myc in tumorigenesis by inhibiting c-Myc-induced apoptosis via INK4a/ARF. *Genes Dev.* 1999;13: 2678-2690.
10. Jacobs JJ, Kieboom K, Marino S, et al. The oncogene and polycomb-group gene bmi-1 regulates cell proliferation and senescence through the ink4a locus. *Nature.* 1999;397:164-168.
11. Lessard J, Sauvageau G. Bmi-1 determines the proliferative capacity of normal and leukaemic stem cells. *Nature.* 2003;423:255-260.
12. Glinsky GV, Berezovska O, Glinskii AB. Microarray analysis identifies a death-from-cancer signature predicting therapy failure in patients with multiple types of cancer. *J Clin Invest.* 2005;115:1503-1521.
13. Kang MK, Kim RH, Kim SJ, et al. Elevated Bmi-1 expression is associated with dysplastic cell transformation during oral carcinogenesis and is required for cancer cell replication and survival. *Br J Cancer.* 2007;96:126-133.
14. Dukers DF, van Galen JC, Giroth C, et al. Unique polycomb gene expression pattern in Hodgkin's lymphoma and Hodgkin's lymphoma-derived cell lines. *Am J Pathol.* 2004;164:873-881.
15. Raaphorst FM, Vermeer M, Fieret E, et al. Site-specific expression of polycomb-group genes encoding the HPC-HPH/PRC1 complex in clinically defined primary nodal and cutaneous large B-cell lymphomas. *Am J Pathol.* 2004;164:533-542.
16. Kim JH, Yoon SY, Jeong SH, et al. Overexpression of Bmi-1 oncoprotein correlates with axillary lymph node metastases in invasive ductal breast cancer. *Breast.* 2004; 13:383-388.
17. Silva J, Garcia JM, Pena C, et al. Implication of polycomb members Bmi-1, Mel-18, and Hpc-2 in the regulation of p16INK4a, p14ARF, h-TERT, and c-Myc expression in primary breast carcinomas. *Clin Cancer Res.* 2006;12:6929-6936.
18. Vonlanthen S, Heighway J, Altermatt HJ, et al. The bmi-1 oncoprotein is differentially expressed in non-small cell lung cancer and correlates with INK4A-ARF locus expression. *Br J Cancer.* 2001;84:1372-1376.
19. Breuer RH, Snijders PJ, Smit EF, et al. Increased expression of the EZH2 polycomb group gene in BMI-1-positive neoplastic cells during bronchial carcinogenesis. *Neoplasia.* 2004;6:736-743.
20. Vrzalikova K, Skarda J, Ehrmann J, et al. Prognostic value of Bmi-1 oncoprotein expression in NSCLC patients: a tissue microarray study. *J Cancer Res Clin Oncol.* 2008; 134:1037-1042.
21. Varambally S, Dhanasekaran SM, Zhou M, et al. The polycomb group protein EZH2 is involved in progression of prostate cancer. *Nature.* 2002;419:624-629.
22. Kleer CG, Cao Q, Varambally S, et al. EZH2 is a marker of aggressive breast cancer and promotes neoplastic transformation of breast epithelial cells. *Proc Natl Acad Sci USA.* 2003;100:11606-11611.
23. Bachmann IM, Halvorsen OJ, Collett K, et al. EZH2 expression is associated with high proliferation rate and aggressive tumor subgroups in cutaneous melanoma and cancers of the endometrium, prostate, and breast. *J Clin Oncol.* 2006;24:268-273.
24. Weikert S, Christoph F, Kollermann J, et al. Expression levels of the EZH2 polycomb transcriptional repressor correlate with aggressiveness and invasive potential of bladder carcinomas. *Int J Mol Med.* 2005;16:349-353.
25. Sudo T, Utsunomiya T, Mimori K, et al. Clinicopathological significance of EZH2 mRNA expression in patients with hepatocellular carcinoma. *Br J Cancer.* 2005;92:1754-1758.
26. Matsukawa Y, Semba S, Kato H, et al. Expression of the enhancer of zeste homolog 2 is correlated with poor prognosis in human gastric cancer. *Cancer Sci.* 2006;97:484-491.
27. Glinsky GV. "Stemness" genomics law governs clinical behavior of human cancer: implications for decision making in disease management. *J Clin Oncol.* 2008;26:2846-2853.
28. American Joint Committee on Cancer. Lung. In: Beahrs OH, Henson DE, Hutter RVP, Kennedy BJ, eds. AJCC Manual for Staging of Cancer. Philadelphia: Lippincott; 1992: 115-122.
29. Ougolkov AV, Bilim VN, Billadeau DD. Regulation of pancreatic tumor cell proliferation and chemoresistance by the histone methyltransferase enhancer of zeste homologue 2. *Clin Cancer Res.* 2008;14:6790-6796.
30. Su IH, Dobenecker MW, Dickinson E, et al. Polycomb group protein ezh2 controls actin polymerization and cell signaling. *Cell.* 2005;121:425-436.
31. Raaphorst FM, van Kemenade FJ, Blokzijl T, et al. Coexpression of BMI-1 and EZH2 polycomb group genes in Reed-Sternberg cells of Hodgkin's disease. *Am J Pathol.* 2000;157:709-715.
32. Song LB, Zeng MS, Liao WT, et al. Bmi-1 is a novel molecular marker of nasopharyngeal carcinoma progression and immortalizes primary human nasopharyngeal epithelial cells. *Cancer Res.* 2006;66:6225-6232.
33. Hommura F, Dosaka-Akita H, Mishina T, et al. Prognostic significance of p27KIP1 protein and ki-67 growth fraction

in non-small cell lung cancers. *Clin Cancer Res.* 2000;6:4073-4081.
34. Mishina T, Dosaka-Akita H, Hommura F, et al. Cyclin E expression, a potential prognostic marker for non-small cell lung cancers. *Clin Cancer Res.* 2000;6:11-16.
35. Bracken AP, Pasini D, Capra M, et al. EZH2 is downstream of the pRB-E2F pathway, essential for proliferation and amplified in cancer. *EMBO J.* 2003;22:5323-5335.
36. Tang X, Milyavsky M, Shats I, et al. Activated p53 suppresses the histone methyltransferase EZH2 gene. *Oncogene.* 2004;23:5759-5769.
37. Hussain M, Rao M, Humphries AE, et al. Tobacco smoke induces p-polycomb-mediated repression of Dickkopf-1 in lung cancer cells. *Cancer Res.* 2009;69:3570-3578.
38. Cao Q, Yu J, Dhanasekaran SM, et al. Repression of E-cadherin by the polycomb group protein EZH2 in cancer. *Oncogene.* 2008;27:7274-7284.
39. Fujii S, Ochiai A. Enhancer of zeste homolog 2 downregulates E-cadherin by mediating histone H3 methylation in gastric cancer cells. *Cancer Sci.* 2008;99:738-746.
40. Yu J, Cao Q, Mehra R, et al. Integrative genomics analysis reveals silencing of beta-adrenergic signaling by polycomb in prostate cancer. *Cancer Cell.* 2007;12:419-431.
41. Tan J, Yang X, Zhuang L, et al. Pharmacologic disruption of polycomb-repressive complex 2-mediated gene repression selectively induces apoptosis in cancer cells. *Genes Dev.* 2007;21:1050-1063.
42. Liu JH, Song LB, Zhang X, et al. Bmi-1 expression predicts prognosis for patients with gastric carcinoma. *J Surg Oncol.* 2008;97:267-272.
43. Wang H, Pan K, Zhang HK, et al. Increased polycomb-group oncogene Bmi-1 expression correlates with poor prognosis in hepatocellular carcinoma. *J Cancer Res Clin Oncol.* 2008;134:535-541.
44. Qin ZK, Yang JA, Ye YL, et al. Expression of Bmi-1 is a prognostic marker in bladder cancer [serial online]. *BMC Cancer.* 2009;9:61.
45. Engelsen IB, Mannelqvist M, Stefansson IM, et al. Low BMI-1 expression is associated with an activated BMI-1-driven signature, vascular invasion, and hormone receptor loss in endometrial carcinoma. *Br J Cancer.* 2008;98:1662-1669.
46. Arnes JB, Collett K, Akslen LA. Independent prognostic value of the basal-like phenotype of breast cancer and associations with EGFR and candidate stem cell marker BMI-1. *Histopathology.* 2008;52:370-380.
47. Bachmann IM, Puntervoll HE, Otte AP, Akslen LA. Loss of BMI-1 expression is associated with clinical progress of malignant melanoma. *Mod Pathol.* 2008;21:583-590.
48. Yonemitsu Y, Imazeki F, Chiba T, et al. Distinct expression of polycomb group proteins EZH2 and BMI1 in hepatocellular carcinoma. *Hum Pathol.* 2009;40:1304-1311.
49. Pietersen AM, Horlings HM, Hauptmann M, et al. EZH2 and BMI1 inversely correlate with prognosis and TP53 mutation in breast cancer. *Breast Cancer Res.* 2008;10:R109.

INTERNAL MEDICINE

□ CASE REPORT □

Primary Mediastinal Liposarcoma, with 6 Years of Follow-up to Autopsy, Revealed Histopathological Features of Primary and Metastatic Lesions

Satoshi Konno[1], Satoshi Oizumi[1], Naofumi Shinagawa[1], Eiki Kikuchi[1], Jun Konishi[1], Kenichiro Ito[1], Nobuyuki Hizawa[2], Akihiro Takiyama[3], Shinya Tanaka[3] and Masaharu Nishimura[1]

Abstract

Primary mediastinal liposarcoma was observed in a 73-year-old man. Because of tight adhesions to adjacent tissues, neither complete resection nor surgical debulking of the tumor was possible. A T-tube was inserted into the patient's trachea for severe dyspnea, and he was treated with radiotherapy and an oral peroxisome proliferator-activated receptor-γ agonist. The patient died 6 years after the initial diagnosis. Autopsy revealed liposarcoma composed of 3 subtypes in the primary tumor: well-differentiated, dedifferentiated, and round cell components. Round cell and dedifferentiated liposarcomas were predominantly observed in the metastatic nodules.

Key words: mediastinal liposarcoma, primary, metastasis, autopsy, radiotherapy

(Inter Med 49: 771-775, 2010)
(DOI: 10.2169/internalmedicine.49.2974)

Introduction

Liposarcoma is the most common type of soft tissue sarcoma, occurring in the lower extremities and retroperitoneum (1). Primary mediastinal liposarcoma is rare and thought to represent less than 1% of all mediastinal tumors (2). Because of its lower frequency, the clinical features of primary mediastinal liposarcoma remain unclear, and hence, standard therapeutic strategies for this tumor have not yet been established. Here, we report an autopsy case of unresectable primary mediastinal liposarcoma that we followed for 6 years from the initial diagnosis, and we present the histopathological findings of the primary and metastatic lesions observed at autopsy. In the present case, 3 different histological findings (well-differentiated, dedifferentiated, and round cell type components) were observed in the primary tumor, and the dedifferentiated and round cell components were predominantly observed in the metastatic lesions. This is the first case of unresectable primary mediastinal liposarcoma that was followed to autopsy, which revealed the histopathological features of the primary and various metastatic lesions.

Case Report

A 73-year-old man presented with a 6-month history of gradually progressive, nonproductive cough and inspiratory dyspnea in November 2000. On admission, he had stridor in both expiratory and inspiratory phases of respiration. On computed tomography (CT), a large tumor was located in the midline posterior mediastinum, extending into the neck through the thoracic inlet and into the anterior portion of the left atrium. Large, homogenous, fat-dense regions were identified at the thoracic inlet level and at the level of the subcarina (Fig. 1a, 1b). The lesion in the thoracic inlet level

[1]The First Department of Medicine, Hokkaido University School of Medicine, Sapporo, [2]Division of Respiratory Medicine, Institute of Clinical Medicine, University of Tsukuba, Tsukuba and [3]Laboratory of Cancer Research, Department of Pathology, Hokkaido University Graduate School of Medicine, Sapporo
Received for publication October 5, 2009; Accepted for publication December 27, 2009
Correspondence to Dr. Satoshi Konno, satkonno@med.hokudai.ac.jp

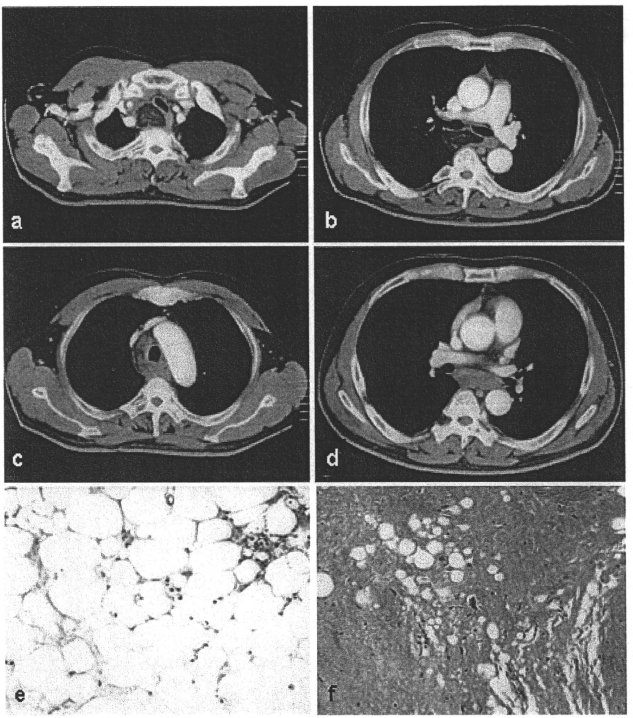

Figure 1. Computed tomography (CT) findings on initial admission at the thoracic inlet level (a), at the subcarina level (b), region between a and b (c), and at the left atrium level (d). Microscopic features of the well-differentiated liposarcoma lesion (Hematoxylin and Eosin staining ×200) (e) and the dedifferentiated liposarcoma lesion (Hematoxylin and Eosin staining ×100) (f).

compressed the trachea. Solid regions were detected between these 2 fat-dense regions (Fig. 1c) and at the level of the left atrium (Fig. 1d). Magnetic resonance imaging (MRI) showed a high signal intensity on both T1- and T2-weighted images at the thoracic inlet level and at the level of the subcarina (Figure not shown). Regions corresponding to Fig. 1c and Fig. 1d included a mixture of high and low signal intensities on both T1- and T2-weighted images (Figure not shown). Brain and abdominal CT scans showed no metastatic lesions.

Based on the CT and MRI findings, primary mediastinal liposarcoma was strongly suspected. The patient underwent surgery for possible complete resection or surgical debulking to relieve dyspnea. Gross examination showed that the tumor was encapsulated, extending from the neck to the anterior portion of the heart. Neither complete resection nor debulking of the tumor was possible because it adhered tightly to adjacent structures, especially to the membranous portion of the trachea and esophagus. Histopathological examination of the biopsy specimens obtained from the homogenous fat-dense regions (corresponding to the levels shown on the CT scan in Fig. 1a, 1b) revealed a well-differentiated type of liposarcoma characterized by mature adipoid tissues with various sized fatty droplets, including bizarre, nucleated lipoblasts (Fig. 1e). On the other hand, a biopsy specimen of the solid regions (corresponding to the level shown in Fig. 1c, 1d) revealed a dedifferentiated liposarcoma composed of sarcomatous tissue with dense collagenous tissue (Fig. 1f).

In April 2001, 3 months after the surgical procedure, the patient was urgently admitted to our hospital because of severe dyspnea. CT images revealed narrowing of the trachea caused by further enlarged tumor. Tracheostomy was performed with the insertion of a silicon T-tube (13.0-mm internal diameter), and his dyspnea improved. Subsequently, the patient received radiotherapy to the tumor, from the neck

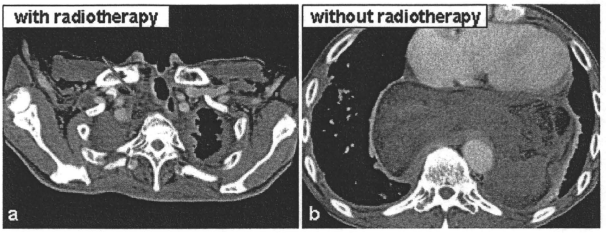

Figure 2. CT findings 2 months before death. The part of the tumor receiving radiotherapy (arrow) (a) and the part that did not receive radiotherapy (b).

to a point 3 cm below the carina, for a total dose of 30 Gy in 12 fractions over a 3-week period. Furthermore, prescription of a peroxisome proliferator-activated receptor-γ (PPAR-γ) agonist, pioglitazone, in expectation of differentiation of the liposarcoma, was started (at a single daily dose of 800 mg, orally) in February 2002. Pleural effusions on the right and left sides were observed in October 2002 and September 2003, respectively. The effusion on the right side did not increase further after repeated drainage procedures, and pleurodesis with OK-432 10KE was effective on the left side. Although the part of the tumor receiving radiotherapy was well controlled (Fig. 2a), the remaining tumor behind the heart, without radiotherapy, increased gradually (Fig. 2b). In April 2007, about 6 years after the initial diagnosis, the patient died of heart failure and pneumonia.

Autopsy examination revealed a large tumor localized in the posterior part of the mediastinum extending to the neck and to the anterior portion of the heart. Behind the heart, the main tumor mass, 17×11 cm in size (Fig. 3a), was observed, corresponding to the abnormal density area detected on CT 2 months before the patient's death (Fig. 2b). The tumor had a well-demarcated, lobular appearance composed of both yellowish fatty lesions and a whitish, solid, firm mass. Microscopic examination of the yellowish part (Fig. 3a, portion A) demonstrated a well-differentiated component of liposarcoma (Fig. 3b), whereas the whitish part (Fig. 3a, portion B) possessed the features of dedifferentiated liposarcoma (Fig. 3c). Furthermore, foci of the round cell type of liposarcoma, characterized by uniform round to oval-shaped cells, were present in both areas (Fig. 3d, only the pathological findings from portion B are shown). Multiple metastases were observed in the liver, bilateral lungs, bilateral Gerota's fascia, the left adrenal gland, mesentery, left fifth rib, and the left side of the neck. Microscopically, the metastatic lesions in the liver, lower lobe of the right lung, Gerota's fascia, adrenal gland, and mesentery were mainly composed of a round cell component of liposarcoma (Fig. 3e), while those of the upper lobe of the right lung were mainly composed of a dedifferentiated component (Fig. 3f).

Discussion

Liposarcoma is the most common soft tissue sarcoma, occurring frequently in the lower extremities and retroperitoneum (1). The clinicopathological and prognostic features of liposarcoma arising in the extremities and retroperitoneum have been well reported (1, 3-5). However, documentation in the literature on mediastinal liposarcoma is limited because of its rarity. After the recent statements of the World Health Organization (WHO) classification of soft tissue sarcomas (6), only 2 studies have described primary mediastinal liposarcomas (7, 8). Accordingly, a case report of primary mediastinal liposarcoma is still valuable and, to the best of our knowledge, this is the first report of an unresectable mediastinal liposarcoma detailing the clinical course from initial diagnosis to autopsy and describing the histopathological features of the primary and metastatic lesions.

The histological findings of metastatic liposarcoma arising from a primary in the retroperitoneum have been well-described (9-12). Well-differentiated liposarcoma tends to be low grade and has been reported to have fewer metastases, whereas myxoid/round cell, pleomorphic, and dedifferentiated types of liposarcoma have more aggressive behavior and higher rates of metastases. However, in the case of primary mediastinal liposarcoma, few studies have described the metastatic findings. In particular, after the recent statements of the WHO classification of soft tissue sarcomas (6), only one study, by Hahn and Fletcher, in which 2 of 24 cases showed distant metastases exhibiting dedifferentiated and pleomorphic-like components in each, has addressed this issue (7). In the present case, 3 different histological findings, including well-differentiated, dedifferentiated, and round cell type components, were observed in the primary tumor. In contrast, the dedifferentiated and round cell types were predominantly observed in the metastatic regions, thus suggesting that these 2 histological components have more strong potential for metastasis, as indicated by previous reports on the different origins of this tumor (1, 13, 14).

Surgical excision has been curative for most primary mediastinal liposarcomas, especially well-differentiated ones, despite their large size (15-17). There have also been several

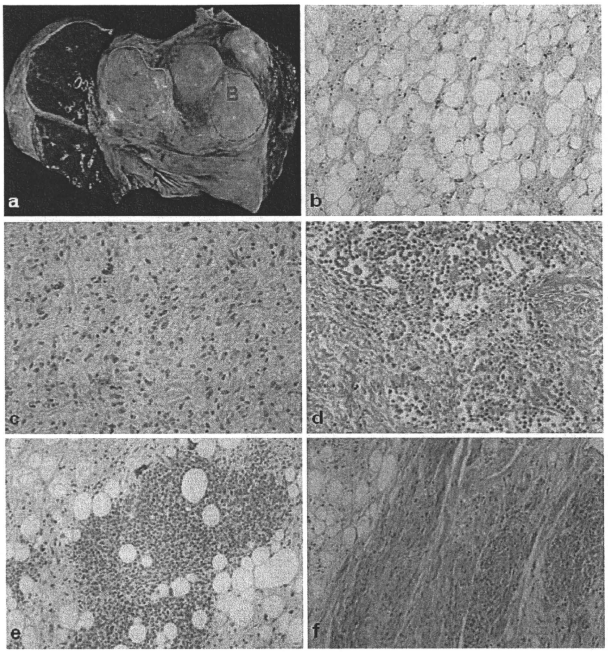

Figure 3. Gross examination (a) at autopsy. The tumor is lobular and consists of a yellowish, fatty mass (portion A) and a whitish, solid, firm mass (portion B). Microscopic features of the yellowish part, the well-differentiated liposarcoma (b, Hematoxylin and Eosin staining ×100), and the whitish part, the dedifferentiated component (c, Hematoxylin and Eosin staining ×200). A round cell type component is included both in portion A and portion B (d, in portion B, Hematoxylin and Eosin staining ×200). The microscopic findings of the metastatic region. Round cell component (e, Hematoxylin and Eosin staining ×100) from the lower right lung lobe, dedifferentiated component (f, Hematoxylin and Eosin staining ×100) from the upper right lung lobe.

reports of very large primary mediastinal liposarcomas that adhered to adjacent tissues (18-20); even in such cases, partial excision usually relieved symptoms related to the compressive effects of the tumor. However, in the present case, tight adhesion to adjacent structures, possibly due to the fibrous environment associated with its variety of histopathological subtypes of liposarcoma, especially in the dedifferentiated subtype, allowed neither complete resection nor even debulking of the tumor. The unresectability of the tumor caused an unfavorable clinical course in this case.

Because of the low incidence of primary mediastinal liposarcomas, treatment strategies are extrapolated from those for similar tumors in other places, particularly for unresectable cases such as the one described in this report. A recent review of a large number of patients with liposarcoma in the extremities suggests the efficacy of postoperative radiotherapy to decrease the local recurrence rate (1). Furthermore, several case reports of mediastinal liposarcoma also suggested the efficacy of postoperative radiotherapy (1, 15, 18). In the present case, it seemed that the part of the tumor that received radiotherapy was well controlled, whereas the rest of the tumor that did not receive radiotherapy progressed, suggesting that radiotherapy might have contributed to local control of the tumor.

It has been reported that the nuclear receptor PPAR-γ plays a central role in adipocyte differentiation (21, 22). Of note, Demetri et al reported 3 cases of liposarcoma in which PPAR-γ agonist administration induced histological and biochemical differentiation in vivo (23). It is difficult to discuss the efficacy of this agent based on the clinical course of this case, but further clinical studies would provide evidence for the efficacy of these agonists in the treatment of this tumor.

In summary, this report describes a case of unresectable primary mediastinal liposarcoma that we followed for 6

years from initial diagnosis to autopsy. Further accumulation of case reports and descriptions of patients with this tumor would help develop standard treatments for this tumor, particularly for unresectable cases, as described in this report.

Acknowledgement

The authors would like to express their sincere gratitude to Dr. Koichi Yamazaki, the former associate professor of the First Department of Medicine, Hokkaido University School of Medicine, who died recently.

References

1. Engstrom K, Bergh P, Gustafson P, et al. Liposarcoma: Outcome based on the Scandinavian Sarcoma Group Register. Cancer **113**: 1649-1656, 2008.
2. Macchiarini P, Ostertag H. Uncommon primary mediastinal tumors. Lancet Oncol **5**: 107-118, 2004.
3. Linehan DC, Lewis JJ, Leung D, Brennan MF. Influence of biologic factors and anatomic site in completely resected liposarcoma. J Clin Oncol **18**: 1637-1683, 2000.
4. Zagars GK, Gostitz MS, Pollack A. Liposarcoma: outcome and prognostic factors following conservation surgery and radiation therapy. Int J Radiation Oncology Biol Phys **36**: 311-319, 1996.
5. Chang HR, Hajdu SI, Collin C, Brennan MF. The prognostic value of histologic subtypes in primary extremity liposarcoma. Cancer **64**: 1514-1520, 1989.
6. Fletcher CDM, Unni KK, Mertens F. World Health Organization Classification of Tumors: Pathology and genetics of tumors of soft tissue and bone. IARC Press, Lyon, 2002: 35-46.
7. Hahn HP, Fletcher CDM. Primary mediastinal liposarcoma: Clinicopathologic analysis of 24 cases. Am J Surg Pathol **31**: 1868-1874, 2007.
8. Hirai S, Hamanaka Y, Mitsui N, Uegami S, Matsuura Y. Surgical resection of primary liposarcoma of the anterior mediastinum. Ann Thorac Cardiovasc Surg **14**: 38-41, 2008.
9. Mussi C, Collini P, Miceli R, et al. The prognostic impact of dedifferentiation in retroperitoneum liposarcoma: a series of surgically treated patients at a single institution. Cancer **113**: 1657-1665, 2008.
10. Huang HY, Brennan MF, Singer S, Antonescu CR. Distant metastatis in retroperitoneal dedifferentiated liposarcoma is rare and rapidly fetal: a clinicopathological study with emphasis on the low-grade myxofibrosarcoma-like pattern as an early sign of dedifferentiation. Modern Patholoy **18**: 976-984, 2005.
11. Fabre-Guillevin E, Coindre JM, Somerhausen NSA, Bonichon F, Stoeckle E, Bui NB. Retroperitoneal liposarcoma: follow-up analysis of dedifferentiation after clinicopathologic reexamination of 86 liposarcomas and malignant fibrous histiocytomas. Cancer **106**: 2725-2733, 2006.
12. Hasegawa T, Seki K, Hasegawa F, et al. Dedifferentiated liposarcoma of retroperitoneum and mesentery: varied growth patterns and histological grades-A clinicopathologic study of 32 cases. Hum Pathol **31**: 717-727, 2000.
13. Sheah K, Ouellette HA, Torriani M, Nielsen GP, Kattapuram S, Bredella MA. Metastatic myxoid liposarcoma: imaging and histopathologic findings. Skeletal Radiol **37**: 251-258, 2008.
14. Chang HR, Hajdu SI, Collin C, Brennan MF. The prognostic value of histologic subtypes in primary extremity liposarcoma. Cancer **64**: 1514-1520, 1989.
15. Klimstra DS, Moran CA, Perino G, Koss MN, Rosai J. Liposarcoma of the anterior mediastinum and thymus: A clinicopathologic study of 28 cases. Am J Surg Pathol **19**: 782-791, 1995.
16. Dogan R, Ayrancioglu K, Aksu O. Primary mediastinal liposarcoma: A report of a case and review of the literature. J Cardio-Thorac Surg **3**: 367-370, 1989.
17. Schweitzer DL, Aguam AS. Primary liposarcoma of the mediastinum: report of a case and review of the literature. J Thorac Cardiovasc Surg **74**: 83-97, 1977.
18. Grewal RG, Prager K, Austin JHM, Rotterdam H. Long-term survival in non-encapsulated primary liposarcoma of the mediastinum. Thorax **48**: 1276-1277, 1993.
19. Eisenstat R, Bruce D, Williams LE, Katz DS. Primary liposarcoma of the mediastinum with coexistent mediastinal lipomatosis. Am J Roentgenol **174**: 572-573, 2000.
20. Jung JI, Kim H, Kang SW, Park SH. Radiological findings in myxoid liposarcoma of the anterior mediastinum. Br J Radiol **71**: 975-976, 1998.
21. Tontonoz P, Hu E, Spiegelma BM. Stimulation of adipogenesis in fibroblasts by PPAR gamma 2, a lipid-activated transcription factor. Cell **9**: 1147-1156, 1994.
22. Tontonoz P, Singer S, Forman BM, et al. Terminal differentiation of human liposarcoma cells induced by ligands for peroxisome proliferators-activated receptor γ and the retinoid X receptor. Proc Natl Acad Sci USA 1997 **94**: 237-242, 1997.
23. Demetri GD, Fletcher CDM, Mueller E, et al. Induction of solid tumor differentiation by the peroxisome proliferator-activated receptor-γ agonists troglitazone in patients with liposarcoma. Proc Natl Acad Sci USA **96**: 3951-3956, 1999.

Combination Therapy of Established Tumors by Antibodies Targeting Immune Activating and Suppressing Molecules

Kazuyoshi Takeda,*,† Yuko Kojima,‡ Tomoyasu Uno,§ Yoshihiro Hayakawa,† Michele W. L. Teng,† Hirohisa Yoshizawa,§ Hideo Yagita,* Fumitake Gejyo,§ Ko Okumura,* and Mark J. Smyth†

The blockade of immune suppression against antitumor responses is a particularly attractive strategy when combined with agents that promote tumor-specific CTLs. In this study, we have attempted to further improve the CTL induction and potent antitumor efficacy of a combination mAb-based therapy (termed "trimAb therapy") that comprises tumor cell death-inducing anti-death receptor 5 mAb and immune activating anti-CD40 and anti-CD137 mAbs. Among trimAb-treated tumors, the infiltration of $CD4^+$ $Foxp3^+$ cells was greater in progressing tumors compared with stable tumors. Blockade of CTLA-4 (CD152)-mediated signals by an antagonistic mAb substantially increased the tumor rejection rate of trimAb therapy, although the immune responses of draining lymph node cells were not augmented. Interestingly, by comparison, additional treatment with agonistic anti-glucocorticoid-induced TNF receptor mAb, antagonistic anti-programmed death-1 (CD279) mAb, or agonistic anti-OX40 (CD134) mAb significantly augmented immune responses of draining lymph node cells, but did not augment the therapeutic effect of trimAb. CD4 T cell depletion reduced the antitumor effect of anti–CTLA-4 mAb treatment alone, but did not reduce the tumor rejection rate of trimAb in conjunction with anti–CTLA-4 mAb. Thus, the blockade of the CTLA-4–mediated inhibitory signal in tumor infiltrating CTL may be the most effective strategy to augment the effect of immune therapies that generate tumor-specific CTL. ***The Journal of Immunology*****, 2010, 184: 5493–5501.**

Immunotherapy based on mAbs targeting cancer cells is now developed as a valid approach to treat cancer (1–3); nevertheless, the therapeutic effect is still often relatively low or incomplete. We have previously reported that tumor cell apoptosis induction by anti-death receptor (DR)-5 (TRAIL receptor) mAb exerts a potent antitumor effect in mice (4). Moreover, when this apoptosis-inducing therapy (anti-DR5 mAb treatment) was combined with immune activation (anti-CD40 and anti-CD137 mAb treatment, termed "trimAb"), strong tumor-specific CTLs were promptly induced, resulting in the complete rejection of established tumor in the majority of trimAb treated-mice (5). We believe that the combination therapy of tumor apoptosis induction and immune activation is an attractive approach to treat cancer (6, 7), because trimAb induced complete rejection of a large proportion of fibrosarcomas induced de novo by 3-methylcholanthrene (MCA) and could also reject established tumors containing as many as 90% TRAIL-resistant tumor variants (5). However, the therapeutic effect of trimAb was limited against much larger tumor masses, and trimAb did not achieve a 100% rejection rate.

Suppressive mechanisms in immune responses normally play a critical role in maintaining immune homeostasis. However, these suppressive mechanisms are also considered as one of main reasons for the failure of cancer immunotherapies because they induce peripheral tolerance of tumor-specific immune responses and allow tumor growth (8, 9). $CD4^+$ $CD25^+$ $Foxp3^+$ regulatory T cells have been revealed as the most important population of immune suppressors, and their depletion has been reported to augment antitumor immune responses (10, 11). CTLA-4 (CD152) and glucocorticoid-induced TNF receptor (GITR) were reported as the critical molecules for regulatory T cell function (11–14). CTLA-4–mediated signals also directly inhibit activated T cell functions (15), and thus blockade of CTLA-4–mediated signals has been suggested as a possible strategy to treat cancers (16, 17). Agonistic anti-GITR mAb (DTA-1) treatment was also report to eradicate established tumors (18). Moreover, programmed death-1 (PD-1) –mediated signals were also reported as a critical inhibitory mechanism regulating antitumor immune responses (19, 20). It is expected that inhibitory signals might be augmented as a feedback mechanism when immune responses are enhanced, and thus blockade of inhibitory signals during therapy-induced immune responses to tumor may well augment the therapeutic effect of such tumor-specific T cell-inducing therapies.

Based on our finding that $CD4^+$ $Foxp3^+$ cells preferentially infiltrated in progressing tumor masses, but not stable tumors, of trimAb-treated mice, we have attempted to improve the therapeutic effect of trimAb using a variety of mAbs that block inhibitory pathways. Antagonistic anti–CTLA-4 mAb, but not agonistic anti-GITR mAb or antagonistic anti–PD-1 mAb, substantially increased the cancer rejection rate caused by trimAb treatment. Additional

*Department of Immunology and ‡Division of Biomedical Imaging Research, Biomedical Research Center, Juntendo University School of Medicine, Tokyo; §Division of Respiratory Medicine, Department of Homeostatic Regulation and Development, Graduate School of Medical and Dental Sciences, Niigata University, Niigata, Japan; and †Cancer Immunology Program, Peter MacCallum Cancer Centre, East Melbourne, Victoria, Australia

Received for publication September 14, 2009. Accepted for publication March 12, 2010.

This work was supported by the Ministry of Education, Science, and Culture, Japan (to K.T.), Grant 07-23904 from the Princess Takamatsu Cancer Research Fund (to K.T.), a Grant-in-Aid from the Tokyo Biochemical Research Foundation (to K.T.), a National Health and Medical Research Council of Australia Senior Principal Research Fellowship (to M.J.S.), a Doherty Fellowship (to M.W.L.T.), a Susan G. Komen Breast Cancer Foundation grant (to M.J.S.), and a project grant from the Cancer Council of Victoria (to M.J.S.).

Address correspondence and reprint requests to Dr. Kazuyoshi Takeda, Department of Immunology, Juntendo University School of Medicine, 2-1-1 Hongo, Bunkyo-ku, Tokyo 113-8421, Japan. E-mail address: ktakeda@juntendo.ac.jp

Abbreviations used in this paper: DR, death receptor; GITR, glucocorticoid-induced TNF receptor; MCA, 3-methylcholanthrene; PD-1, programmed death-1.

www.jimmunol.org/cgi/doi/10.4049/jimmunol.0903033

activation of CD4 T cells by agonistic anti-OX40 mAb did not augment therapeutic effect of trimAb. Anti-GITR mAb, anti–PD-1 mAb, and anti-OX40 mAb, but not anti–CTLA-4 mAb, augmented tumor-specific immune responses in the tumor-draining lymph nodes. CD4 T cell depletion did not reduce the improved tumor rejection rate of trimAb caused by additional anti–CTLA-4 mAb treatment. Collectively, blockade of CTLA-4 may be a useful strategy to augment CTL-inducing trimAb therapy possibly due to its direct effect by releasing CTL from suppression in the tumor mass.

Materials and Methods

Mice

BALB/c mice at 6 wk of age were from Charles River Japan (Yokohama, Japan) and The Walter and Eliza Hall Institute of Medical Research (Melbourne, Australia). All mice were maintained under specific pathogen-free conditions and used in accordance with the institutional guidelines of Juntendo University (Tokyo, Japan) and the Peter MacCallum Cancer Centre (East Melbourne, Australia).

Abs and tumors

Agonistic anti-mouse DR5 mAb (MD5-1) (4), agonistic anti-mouse CD40 mAb (FGK45; kindly provided by Dr. Antonius G. Rolink, University of Basel, Basel, Switzerland) (21), agonistic anti-mouse CD137 (4-1 BB) mAb (3H3; kindly provided by Dr. Robert S. Mittler, Emory University, Atlanta, GA) (22), antagonistic anti-mouse CTLA-4 (CD152) mAb (UC10-4F10; kindly provided by Dr. Jeffrey A. Bluestone, University of California, San Francisco, CA) (23), agonistic anti-mouse GITR mAb (DTA-1; kindly provided by Dr. Shimon Sakaguchi, Kyoto University, Kyoto, Japan) (24), antagonistic anti-mouse PD-1 (CD279) mAb (RMP1-14) (25), agonistic anti-mouse OX40 (CD134) mAb (OX86) (26), and anti-mouse CD4 mAb (GK1.5) were prepared and purified in our laboratory as previously described (4, 5). The BALB/c-derived TRAIL-sensitive 4T1 mammary carcinoma and colon 26 (CT26) colon carcinoma were maintained as previously described (4, 5).

Therapy of transplanted s.c. tumors

Mice were inoculated with 2×10^5 4T1 tumor cells s.c. in the hind flank. When tumors developed to a size of ~9 mm^2 (7 d after tumor inoculation), 36 mm^2 (10–12 d after tumor inoculation), or 64 mm^2 (18 d after tumor inoculation), groups of mice were administered i.p. with 100 μg anti-DR5 mAb, anti-CD40 mAb, anti-CD137 mAb, anti–CTLA-4 mAb, anti-GITR mAb, anti–PD-1 mAb, anti-CD134 mAb, control hamster IgG, and/or control rat IgG (Sigma-Aldrich, St. Louis, MO) four times every 4 d. Tumor size was measured periodically with a caliper as the product of two perpendicular diameters (mm^2).

CTL functional analysis in draining lymph node

BALB/c mice were inoculated with 4T1 tumor cells (2×10^5/50 μl) in the left footpad, and mAb therapy commenced 7 d after tumor inoculation. Seven days after a single treatment, mononuclear cells were prepared from the tumor-draining lymph node and incubated with mitomycin C-treated (200 μg/ml for 2 h; Kyowa Hakko, New York, NY) 4T1 or CT26 cells (responder/stimulator = 4:1) for 16 h (4). IFN-γ in the cell-free supernatant was determined by using mouse IFN-γ–specific ELISA kits (OptEIA, BD Biosciences, San Jose, CA) according to the manufacturer's instructions. Cytotoxic activity was tested against 4T1 cells or CT26 cells by a standard 4 h [^{51}Cr]-release assay as previously described (4, 5).

Therapy of MCA-induced primary tumors

BALB/c mice were inoculated s.c. in the hind flank with 200 μg MCA (Sigma-Aldrich) in 0.1 ml corn oil (5, 27). When MCA-induced tumors developed to a size of 9–25 mm^2 (60–120 d after MCA inoculation), groups of mice were administered i.p. with 100 μg anti-DR5 mAb, anti-CD40 mAb, anti-CD137 mAb, anti–CTLA-4 mAb, control hamster IgG, and/or control rat IgG four times every 4 d. Anti-CD4 mAb treatment to deplete CD4 T cells was started 4 d prior to treatment with the therapeutic mAbs and repeated every 4 to 5 d. CD4 T cell depletion was confirmed by flow cytometric analysis. Growth of tumors was monitored over the course of 100–180 d. Tumor size was measured periodically with a caliper as the product of two perpendicular diameters (mm^2).

Histological examination

Progressing, stable (no progressive growth for >7 d), and recurrent (progressive growth >7 d postregression) tumors were removed 7–14 d following treatment. Macroscopically rejected tumors were removed 25–30 d after the last mAb treatment. Three-micrometer cryostat sections were fixed with 20% buffered formalin and stained with H&E (4). Immunofluorescent staining was performed as described previously (28). Post-incubation with biotin-conjugated anti-CD8 mAb (53-6.7), anti-CD4 mAb (RM4-5), anti–Gr-1 mAb (RB6-8C5), anti-CD11b mAb (M1/70) (BD Biosciences), anti-Foxp3 mAb (FJK-16S) (eBioscience, San Diego, CA), or isotype-matched control rat IgG2a (R35-95) or IgG2b (A95-1) (BD Biosciences) for 1 h at 37°C, sections were incubated with Alexa Fluor 488- or Alexa Fluor 594-conjugated streptavidin (Invitrogen, Carlsbad, CA) for 45 min at room temperature and finally counterstained and mounted with Vectashield mounting medium containing DAPI (Vector Laboratories, Burlingame, CA). For double-fluorescence immunostaining, sections were fixed with 8% paraformaldehyde in 0.1 M phosphate buffer (pH 7.4) for 30 min at 4°C and stained following a sequential fluorescent method using an Avidin/Biotin Blocking Kit (Vector Laboratories) according to the manufacturer's instructions (29). The fluorescence images were captured with a Zeiss AxioPlan2 fluorescence microscope equipped with a digital camera (Zeiss, Jena, Germany). To quantify the positive-staining cells, the number of infiltrating $CD8^+$, $CD4^+$ $Foxp3^+$, $CD4^+$ $Foxp3^-$, and Gr-1^+ $CD11b^+$ cells in each section was analyzed using the KS400 Image Analysis system (Zeiss). Three to six typical areas of tumor margin were examined in each specimen, and the numbers of positively stained cells were calculated per field of view (T cells: on ×40 and myeloid cells: on ×20).

Statistical analysis

Statistical analysis was performed by two-sample *t* test for the IFN-γ ELISA, cytotoxicity, and tumor growth data. Significant difference in tumor rejection was determined by the Fisher exact test. All *p* values <0.05 were considered significant.

Results

Accumulation of $CD4^+$ $Foxp3^+$ T cells in progressing 4T1 tumor masses following trimAb therapy

As we previously reported (5), a rational mAb-based therapy combining tumor cell death induction (anti-DR5 mAb-induced apoptosis) and immune activation (anti-CD40 and anti-CD137 mAb-induced CTL induction/activation) eradicated established (~25 mm^2, 10 d after tumor inoculation) TRAIL-sensitive 4T1 tumors; however, not all mice were cured. When we examined progressing, stable, and rejected tumors following trimAb therapy, tumor rejection was confirmed by histological analysis (Fig. 1). Infiltration of CD8 T cells was significantly increased in trimAb-treated stable tumors when compared with control progressing tumors, but not trimAb-treated progressing tumors. By contrast, infiltration of both $CD4^+$ $Foxp3^+$ and $CD4^+$ $Foxp3^-$ T cells significantly decreased in trimAb-treated tumors and that resulted in a significant increase in CD8 T cell/regulatory T cell ratio in trimAb-treated tumors (Fig. 1). Moreover, $CD4^+$ $Foxp3^+$ regulatory T cells were significantly reduced in stable tumors even when compared with trimAb-treated progressing tumors and that resulted in a far greater CD8 T cell/regulatory T cell ratio in trimAb-treated stable tumors. Thus, $CD4^+$ $Foxp3^+$ regulatory T cells that dominantly infiltrate into progressing tumors might promote tumor growth by inhibiting the therapeutic effect of trimAb.

Blockade of CTLA-4 augments the antitumor effect of trimAb therapy

A combination of antagonistic anti–CTLA-4 mAb, agonistic anti-GITR mAb, or antagonistic anti–PD-1 mAb with anti-DR5 mAb inhibited tumor growth more effectively than any monotherapy with each mAb, but tumor rejection was not induced (Fig. 2). Tumor rejection was only induced by trimAb therapy, and the rejection rate was significantly increased when trimAb was combined with anti–CTLA-4 mAb, but not anti-GITR mAb or anti–PD-1 mAb (Fig. 2).

When therapies were commenced at a tumor size of 9 mm^2, trimAb and the combination of trimAb and anti–CTLA-4 mAb induced a greater rate of tumor rejection (~80%), and tumor

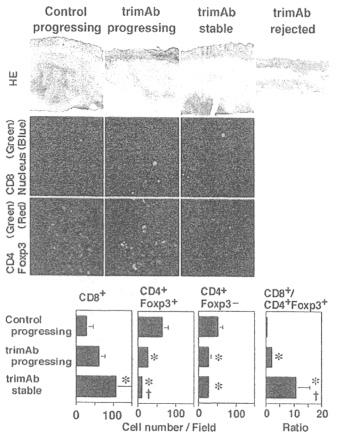

FIGURE 1. Increased $CD8^+$ T cell/$CD4^+$ $Foxp3^+$ T cell ratio in trimAb-treated stable 4T1 tumors. 4T1 tumors were removed from mice and stained with H&E (original magnification ×5), CD8/nucleus (original magnification ×40), or CD4/Foxp3 (original magnification ×40) as described in *Materials and Methods*. The marginal region of s.c. 4T1tumors is shown. Quantification of positive cells in respective sections was shown as a bar graph. Representative photos are presented from three to five mice in each group. $*p < 0.05$ as compared with control progressing tumor; $^{\dagger}p < 0.05$ as compared with trimAb-treated progressing tumor.

growth was significantly inhibited by trimAb or trimAb with anti–CTLA-4 mAb treatment when compared with control or anti–CTLA-4 mAb treatment alone (Fig. 3*A*). Although 4T1 tumors of 64 mm^2 were not rejected by trimAb therapy, additional anti–CTLA-4 mAb treatment significantly inhibited tumor growth at some time points (days 28–34) and achieved complete tumor rejection in a small number of mice (Fig. 3*B*). By contrast, when trimAb therapy was combined with anti-GITR mAb or anti–PD-1 mAb against 9 mm^2 or 64 mm^2 tumors, no effect greater than trimAb therapy alone was observed (data not shown). We did not detect any metastatic nodules in the lungs and livers of the mice that had rejected s.c. primary 4T1 tumors by mAb treatments (data not shown). Thus, CTLA-4 is the preferred target molecule among those examined when blocking immune suppression in the context of the trimAb therapy.

Combination with anti-OX40 mAb treatment did not significantly augment the antitumor effect of trimAb

We have reported that CTL induction/activation and the therapeutic effect of trimAb did not depend on CD4 T cells (5), and therefore activation of Th CD4 cells is an alternative strategy to further augment the therapeutic effect of trimAb. It is thought that OX40-mediated signals increase helper function due to preferential expression of OX40 on CD4 T cells (30). Treatment with anti-OX40 mAb alone slightly but significantly inhibited tumor growth, but only when the treatment commenced against tumors as small as 9 mm^2 in size (Fig. 4). TrimAb and trimAb with anti-OX40 mAb-induced tumor rejection when treatments were commenced against 9 mm^2 and 25 mm^2 4T1 tumors, and both treatments significantly inhibited tumor growth when compared with control or anti-OX40 therapy alone. However, additional agonistic anti-OX40 mAb treatment did not augment the rejection rate or inhibitory effect of trimAb on tumor growth (Fig. 4).

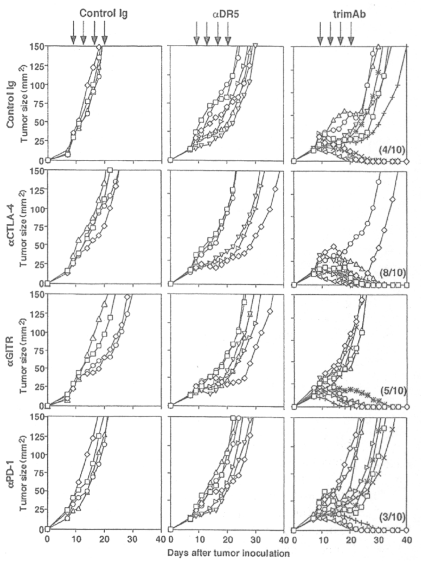

	rejection rate
trimAb + Control Ig	4/10 2/5 2/5 3/6 : 11/26
trimAb + αCTLA-4	8/10 4/5 3/5 4/6 : 19/26 *
trimAb + αGITR	5/10 2/5 2/5 2/5 : 11/25
trimAb + αPD-1	3/10 2/5 2/5 3/6 : 10/26

FIGURE 2. Therapeutic effect of trimAb combined with the mAbs that target immune suppressing pathways. When s.c. 4T1 tumors were 25–36 mm^2 size (10 d after tumor inoculation), mice were treated with control Igs, anti-DR5 mAb, or trimAb (anti-DR5, anti-CD40, and anti-CD137 mAbs) and additionally with control Ig, anti–CTLA-4 mAb, anti-GITR mAb, or anti–PD-1 mAb, as indicated by the arrows. Tumor sizes of individual mice are presented, and tumor rejection rates are indicated in parentheses. Similar results were obtained in four independent experiments including the one depicted, and tumor rejection rates in these are indicated below. $*p < 0.05$ as compared with other groups.

CTL activity in the tumor draining lymph node was not augmented by anti–CTLA-4 mAb treatment

Consistent with our previous report (5), draining lymph node cells of 4T1 tumor-bearing mice treated with trimAb significantly produced IFN-γ when stimulated with 4T1 tumor cells, but not CT26 tumor cells, ex vivo (Fig. 5*A*). IFN-γ production did not correlate with the tumor growth following trimAb or trimAb plus anti–CTLA-4 mAb therapy, indicating that the different response of tumors to the therapies in individual mice was not due to different level of immune activation in tumor draining lymph node by the treatments. Interestingly, additional anti–CTLA-4 mAb treatment did not increase IFN-γ production by draining lymph node cells in trimAb-treated mice; however, additional treatment with anti-GITR mAb, anti–PD-1 mAb, or anti-OX40 mAb significantly augmented IFN-γ production. TrimAb induced specific cytotoxic activity against 4T1 cells, and additional anti-OX40 mAb treatment, but not other mAb treatments, slightly but significantly augmented this specific cytotoxicty (Fig. 5*B*). Neither IFN-γ production nor cytotoxic activity was observed when CD8 T cells were depleted (data not shown). Cytotoxic activity was not

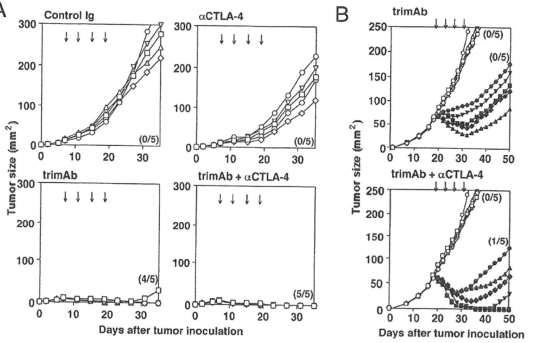

	rejection rate
Control Ig	0/5 0/5 0/5 : 0/15
αCTLA-4	0/5 0/5 0/5 : 0/15
trimAb + Control Ig	4/5 4/5 3/5 : 11/15*
trimAb + αCTLA-4	5/5 4/5 3/5 : 12/15*

	rejection rate
trimAb + Control Ig	0/5 0/5 0/5 : 0/15
trimAb + αCTLA-4	1/5 0/5 1/5 : 2/15

FIGURE 3. Augmented therapeutic effect of trimAb by combination with anti–CTLA-4 mAb. When s.c. 4T1 tumors were 9 mm^2 in size (~7 d after tumor inoculation) (*A*) or 64 mm^2 in size (~18 d after tumor inoculation) (*B*), mice were treated with trimAb (anti-DR5, anti-CD40, and anti-CD137 mAbs), control Ig, or anti–CTLA-4 mAb, as indicated by the arrows. *A*, Tumor sizes of individual mice are presented, and tumor rejection rates are indicated in parentheses. Similar results were obtained in three independent experiments including the one depicted, and tumor rejection rates in these are indicated below. Tumor growth was significantly inhibited by trimAb or trimAb + anti–CTLA-4 mAb treatment when compared with control Ig or anti–CTLA-4 mAb treatment ($p < 0.05$). *B*, Tumor sizes of individual mice are presented, and tumor rejection rates are indicated in parentheses. Open symbols, control Igs; closed symbols, trimAb or trimAb + anti–CTLA-4 mAb as indicated. Similar results were obtained in three independent experiments including the one depicted, and tumor rejection rates in these are indicated below. Tumor growth was significantly inhibited by trimAb + anti-CTLA-4 mAb treatment when compared with trimAb treatment from days 28–34 ($p < 0.05$). *$p < 0.05$ as compared with the groups of mice treated with control Ig or anti–CTLA-4 mAb.

observed against CT26 tumor cells (data not shown). When lymph node cells were prepared 4 d after a single treatment or 4–7 d after a second treatment, similar results were obtained (data not shown). Thus, anti-GITR mAb, anti-OX40 mAb, or anti–PD-1 mAb treatment was more effective at increasing tumor-specific immune responses of the draining lymph node cells in trimAb-treated mice compared with anti–CTLA-4 mAb treatment.

Increased CD4 T cell infiltration by additional anti-GITR mAb or anti-OX40 mAb treatment in stable tumors

In trimAb and anti-GITR mAb-treated stable 4T1 tumors, despite no differences in the number of infiltrating CD8 T cells, the CD8 T cell/regulatory T cell ratio was significantly decreased due to a significant increase in infiltrating $CD4^+$ $Foxp3^+$ T cells (Fig. 6). Interestingly, additional anti-OX40 mAb treatment significantly augmented the infiltration of both $CD4^+$ $Foxp3^+$ T cells and $CD4^+$ $Foxp3^-$ T cells. Additional anti–PD-1 mAb treatment did not significantly modify the number of CD8 T cells, $CD4^+$ $Foxp3^+$ T cells, or $CD4^+$ $Foxp3^-$ T cells or the CD8 T cell/regulatory T cell ratio in stable 4T1 tumors. Additional anti–CTLA-4 mAb treatment appeared to increase the infiltration of $CD8^+$ T cells and the CD8 T cell/regulatory T cell ratio, but these changes were not significant.

Augmentation of the antitumor effect of trimAb by anti–CTLA-4 mAb against MCA-induced sarcoma following CD4 T cell depletion

We then examined the additional effect of anti–CTLA-4 mAb treatment on trimAb therapy against established MCA-induced primary tumors. Anti–CTLA-4 mAb treatment alone significantly inhibited tumor growth but did not induce tumor rejection, and CD4 T cell depletion reduced this antitumor effect of anti–CTLA-4 treatment (Fig. 7), suggesting that effect of antagonistic anti–CTLA-4 mAb alone is possibly mediated by inhibition of CD4 regulatory T cell function, consistent with CTLA-4 reported as a critical effector molecule expressed on regulatory T cells (12).

TrimAb therapy eradicated MCA-induced primary tumors in some mice as we previously reported (5), and the rejection rate was significantly augmented by the combination with anti–CTLA-4 mAb treatment (Fig. 7). CD4 T cell depletion did not decrease the tumor rejection rate induced by trimAb therapy as we previously reported (5), suggesting that trimAb did not require CD4-positive cells to reject tumors, although the early response to trimAb therapy (days 0–10 after the first treatment) was reduced, and tumor rejection was delayed. Interestingly, additional anti–CTLA-4 mAb treatment increased the tumor rejection rate of trimAb in CD4 T cell-depleted mice similar to that in CD4 T cell-intact mice, indicating that anti–CTLA-4 mAb treatment enhanced the tumor rejection rate caused by trimAb independently of CD4 T cells. Thus, augmentation of therapeutic effect of trimAb by antagonistic anti–CTLA-4 mAb appears to be primarily mediated by the relief of direct suppression on CTL.

Immunohistochemistry demonstrated a significant increase in the CD8 T cell/regulatory T cell ratio in stable tumors, due to significantly less infiltration of $CD4^+$ $Foxp3^+$ T cells when compared with that observed in the progressing tumors following either trimAb or trimAb + anti–CTLA-4 mAb treatment (Fig. 8). CD8 T cells, $CD4^+$ $Foxp3^+$ T cells, and $CD4^+$ $Foxp3^-$ T cells increased in the trimAb-treated recurrent tumors compared with stable tumors. When compared with similarly responding tumors treated with trimAb alone, additional anti–CTLA-4 mAb treatment did not alter the number of infiltrating $CD4^+$ $Foxp3^+$ T cells or $CD4^+$ $Foxp3^-$ T cells either in progressing or stable tumors. However, $CD8^+$ T cells were significantly increased by additional

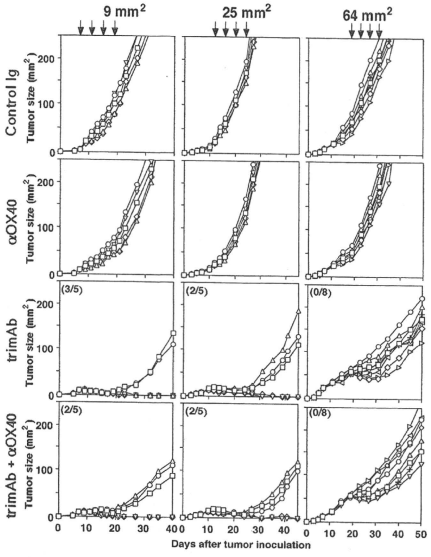

	9 mm²	25 mm²	64 mm²
trimAb + Control Ig	3/5 2/5 6/10 : 11/20	2/5 3/5 3/8 : 8/18	0/8 0/5 0/5 : 0/18
trimAb + αOX40	2/5 3/5 8/10 : 13/20	2/5 2/5 4/8 : 8/18	0/8 0/5 0/5 : 0/18

FIGURE 4. Effect of anti-OX40 mAb on trimAb therapy. When s.c. 4T1 tumors were ~9 mm², 25 mm², or 64 mm² in size, mice were treated with trimAb (anti-DR5, anti-CD40, and anti-CD137 mAbs), control Ig, or anti-OX40 mAb, as indicated by the arrows. Tumor sizes of individual mice are presented, and tumor rejection rates are indicated in parentheses. Similar results were obtained in three independent experiments including the one depicted, and tumor rejection rates in these are indicated below. Anti-OX40 mAb treatment significantly inhibited tumor growth compared with control Ig treatment when treatments were commenced against 9 mm² 4T1 tumors ($p < 0.05$), and trimAb or trimAb + anti-OX40 mAb treatment significantly inhibited tumor growth compared with control Ig or anti-OX40 mAb treatment when treatments were commenced against 9 mm² or 25 mm² 4T1 tumors ($p < 0.05$).

anti–CTLA-4 mAb treatment in both stable and progressing tumors when compared with similarly responding tumors treated with trimAb alone. These observations support the likelihood that anti–CTLA-4 mAb treatment directly effects CD8 T cells in the context of trimAb therapy.

Increased infiltration in myeloid-derived suppressor cells in progressing tumors

$Gr1^+$ $CD11b^+$ myeloid-derived cells and regulatory $CD4^+$ $Foxp3^+$ T cells are now implicated in the suppression of antitumor immune responses (31–33). Moreover, $Gr1^+$ $CD11b^+$ myeloid-derived cells might acquire immune-suppressing function from TGF-β produced by $CD4^+$ $Foxp3^+$ T cells (34) or might either generate or expand tumor-induced regulatory T cells (35, 36), indicating a potential cross-talk between these immune suppressing cells in the tumor mass. Thus, we finally examined the infiltration of $Gr1^+$ $CD11b^+$ cells in MCA-induced tumors (Fig. 9). Infiltrating $Gr1^+$ $CD11b^+$ cells were dramatically reduced in stable tumors,

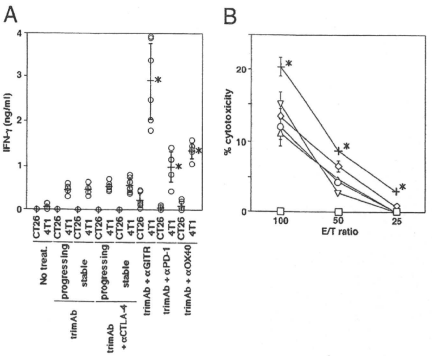

FIGURE 5. CTL response in the draining lymph nodes of mAb-treated tumor-bearing mice. Mononuclear cells were prepared from the draining lymph node of tumor-bearing mice 7 d after a single treatment with the indicated mAbs. *A*, Cells were coincubated with 4T1 tumor cells or CT26 tumor cells, and IFN-γ levels in the cell free supernatant were analyzed by ELISA. Results of four to six individual mice, and the mean ± SD (cross and bar) of those in each group are presented. *B*, Cytotoxic activity of fresh isolated draining lymph node cells was examined against 4T1 tumor cells; no treatment (square), trimAb (circle), trimAb + anti–CTLA-4 mAb (triangle), trimAb + anti-GITR mAb (inverted triangle), trimAb + anti–PD-1 mAb (diamond), and trimAb + anti-OX40 mAb (cross). Data are represented as the mean ± SD of triplicate samples. Similar results were obtained from three independent experiments. $*p < 0.05$ as compared with trimAb-treated mice.

but a number of $Gr1^+$ $CD11b^+$ cells were still observed even when the mice were treated with trimAb and anti–CTLA-4 mAb. $Gr1^+$ $CD11b^+$ cells in the trimAb-treated recurrent tumors were significantly less when compared with trimAb-treated progressing tumors, but significantly more when compared with trimAb-treated stable tumors. Interestingly, additional anti–CTLA-4 mAb treatment significantly reduced the number of $Gr1^+$ $CD11b^+$ cells in the progressing tumors when compared with trimAb-treated progressing tumors (Fig. 9), whereas the number of $CD4^+$ $Foxp3^+$ T cells was comparable (Fig. 8).

Discussion

Induction of tumor-specific CTL is thought to be a critical requirement for effective cancer immunotherapy, and thus improving the ability to induce and sustain effector CTL has been primary focus for the clinical application (37, 38). We have previously reported a triple mAb-based therapy that induces both tumor cell apoptosis and tumor-specific CTL as an effective strategy that can induce complete rejection of a significant proportion of established experimental and de novo tumors (5). However, immunological suppressor cells, particularly regulator T cells and $Gr1^+$ $CD11b^+$ cells, have been implicated to prevent effective tumor-specific immune responses prior to and following immunotherapies (10, 11, 31–33). Therefore, in this study, we examined the contribution of relevant immune-suppressing pathways that might hinder the effectiveness of CTL-inducing trimAb therapy.

Histological analyses showed that $CD4^+$ $Foxp3^+$ cells and $Gr1^+$ $CD11b^+$ cells infiltrated into progressing tumors that resisted trimAb therapy to a similar extent as in untreated mice. This suggested that tumor-infiltrating $CD4^+$ $Foxp3^+$ regulatory T cells and $Gr1^+$ $CD11b^+$ myeloid-derived cells might contribute to tumor